



Investigation on interface-related defects by photoluminescence of cubic (Al)GaN/AlN multi-quantum wells structures



Leonilson K.S. Herval^{a,*}, Marcio P.F. de Godoy^b, Tobias Wecker^c, Donat J. As^c

^a Departamento de Física, Universidade Federal de Lavras (UFLA), Campus Universitário, 37200-000 Lavras, MG, Brazil

^b Departamento de Física, Universidade Federal de São Carlos (UFSCAR), 13560-905 São Carlos, SP, Brazil

^c University of Paderborn, Department of Physics, Warburger Strasse 100, 33098 Paderborn, Germany

ARTICLE INFO

Keywords:

C-GaN
(Al)GaN/AlN
Interface defects
Localization states

ABSTRACT

Cubic (Al)GaN/AlN multiple quantum wells were grown by plasma assisted molecular beam epitaxy with three different configurations at interfaces. We employ temperature-dependent photoluminescence to characterize interface imperfections. Our results show shallow localization states responsible to photocarrier localization at low temperatures. The potential fluctuation model estimates localization energies in the order of few meV. We investigated a single GaN/AlN, double GaN/AlN quantum wells, and a double quantum well with an additional AlGa_xN spacer layer as a step between the wells. The introduction of AlN and AlGa_xN interlayer reduces the effect of localization and indicates better interfaces for the QW structures based on cubic GaN.

1. Introduction

Wide band gap semiconductors have been studied in the last years due the possibilities to operate at higher temperatures thereby expanding their applications in optoelectronics [1] such as the first successful operation of the blue LED [2]. Among many alternatives, group III-Nitrides (Al, In, Ga - N) have excellent applications for solid state lighting, high electron mobility transistors with high saturation velocity and breakdown fields [3]. In this context, (Al)GaN/AlN quantum wells (QW) are attractive as a tunable light emitter in UV optical range. The growth of these materials was intensively investigated in past years and under special conditions, the molecular beam epitaxy allows the growth of high quality thin films of cubic III-nitrides as c-GaN, c-AlN and c-InN as well as their alloys [4–6]. Their crystal symmetry is advantageous due to the absence of internal polarization fields and can be more convenient for some applications as compared to conventional wurtzite structures [7,8] mainly in heterostructures as quantum wells (QW).

In a practical point of view, while spatial confinement allows engineering of electron/hole as well as phonons quantization energies [9], the manner as the interfaces between well and barriers are grown, plays a significant role as a source of localization of carriers. For many applications of GaN-based optoelectronic devices the interface quality affects directly the performance [10]. Photoluminescence measurements (PL) are a standard technique that provides a good way to point out carrier localization due the structural defects or thickness/alloy fluctuations. The optical transitions are very sensitive to interface

effects which act as carriers traps and modify the expected optical behavior.

This work shows the investigation of three kinds of interfaces in (Al)GaN/AlN QW structures and compare to reference bulk sample. Interface defects are explored by means of single QW, double QW with AlN interlayer and step QW with the introduction of AlGa_xN thin layer. Temperature dependent photoluminescence (PL) shows deviation for the expected behavior at low temperatures which are attributed to a consequence of interface defects. Our analysis provides a simple way to estimate the depth of localization as few meV and the advantage of introducing Al(Ga)N interlayers.

2. Experimental

The samples in cubic phase were grown by plasma assisted molecular beam epitaxy (PAMBE) on a substrate consisting of a 10 μm 3C-SiC (001) layer on top of a 500 μm thick Si (001) following the process described in Ref. [11–13]. The cubic GaN is a metastable phase and can only be grown in a narrow window of temperatures in such conditions which can be optimized by in situ monitoring through the reflection high energy electron diffraction (RHEED) [11]. We use a radio frequency plasma source to provide activated nitrogen flux of $2.2 \times 10^{14} \text{ cm}^{-2} \text{ s}^{-1}$ and the gallium was evaporated from Knudsen cells in a flux around $4 \times 10^{14} \text{ cm}^{-2} \text{ s}^{-1}$. The investigated systems were designed for intraband transition devices [14] (not shown in this paper). The structure consists of 100 nm buffer layer of Si-doped c-GaN ($n = 2.10^{18}$

* Corresponding author.

E-mail address: leonilsonk@gmail.com (L.K.S. Herval).

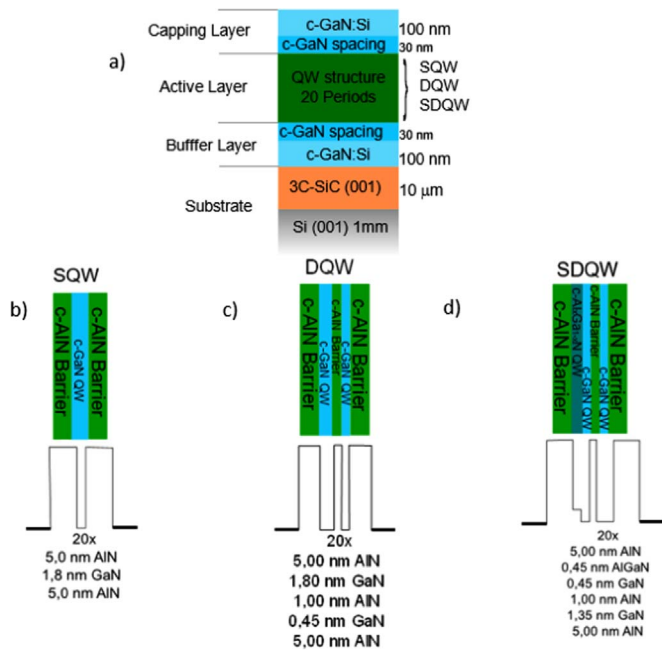


Fig. 1. (a) Standard structure of samples grown by PAMBE. (b) SQW sample: 20 periods of a single quantum well (c) DQW sample: 20 periods of asymmetric quantum wells. (d) SDQW sample: 20 periods of double quantum well, one with a AlGaIn step. Under each design there is the conduction band potential profile.

cm^{-3}) and 30 nm undoped spacing layer to avoid the natural electron diffusion. On top, 20 periods of quantum wells (QW) are grown with 5 nm c-AlN barriers separating each period. The growth was interrupted to evaporate excess metal from the surface (~ 2 min) and during the temperature verification (~ 6 min) after each period. Then the structure is capped with a 30 nm spacing layer and 100 nm of c-GaN Si-doped ($n = 2.10^{18} \text{ cm}^{-3}$) for top contacts. During the growth of all structure, the temperature of substrate was kept at the optimum condition around 720°C as reported in [11].

Our study employs three different structures for the 20 QW as depicted in Fig. 1: i) c-GaN single quantum well (SQW) with 1.8 nm thickness; ii) asymmetric double quantum well (DQW) composed of 1.8 nm c-GaN QW followed by a 1.0 nm of c-AlN barrier and a thin 0.45 nm c-GaN QW; and iii) a step double quantum well (SDQW) which consists of a 0.45 nm step of $\text{c-Al}_{1-x}\text{Ga}_x\text{N}$ followed by a 0.45 nm c-GaN in the first well, a 1.0 nm c-AlN barrier and a 1.35 nm c-GaN well followed by AlN barrier.

The RHEED intensities at (0,0) streak monitored during the growth of 20 QW are shown in Fig. 2. After a temperature adjustment, the Ga shutter is open to grow the GaN well and the RHEED intensity decreases. After the desired thickness, Ga shutter is closed and the intensity restores. When the Al shutter is open for the barrier growth, the RHEED intensity keeps increasing up to the end of such layer growth when the signal is stabilized in the previous maximum before the next period start to be grown. It is notable that the shape is the same for all structures and for the sequence of QW. These results indicate that there are no changing parameters during the growth processes and no

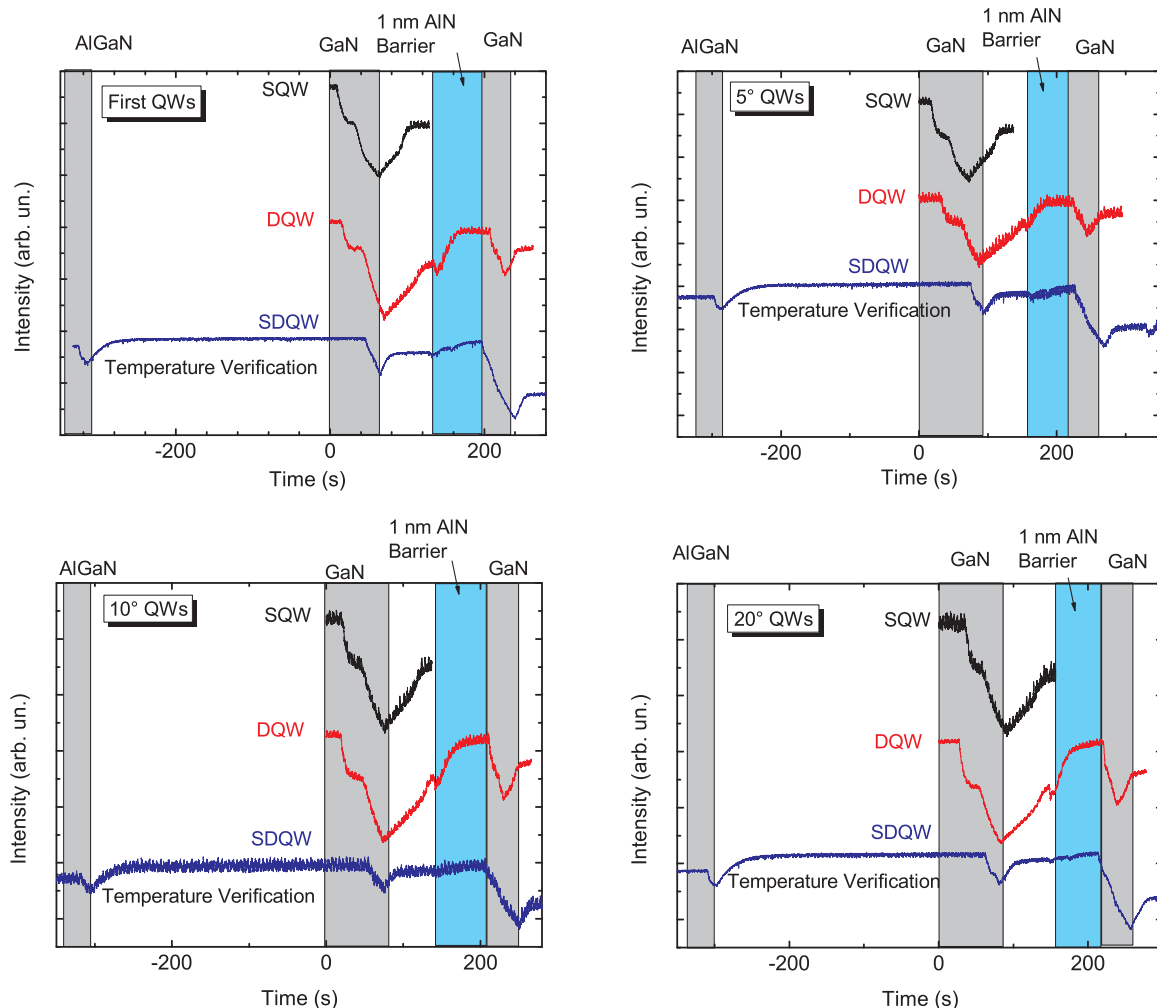


Fig. 2. RHEED intensity during the growth of the QW for the three kinds of samples (SQW, DQW and SDQW) for the first, fifth, tenth and twentieth period of grown process.

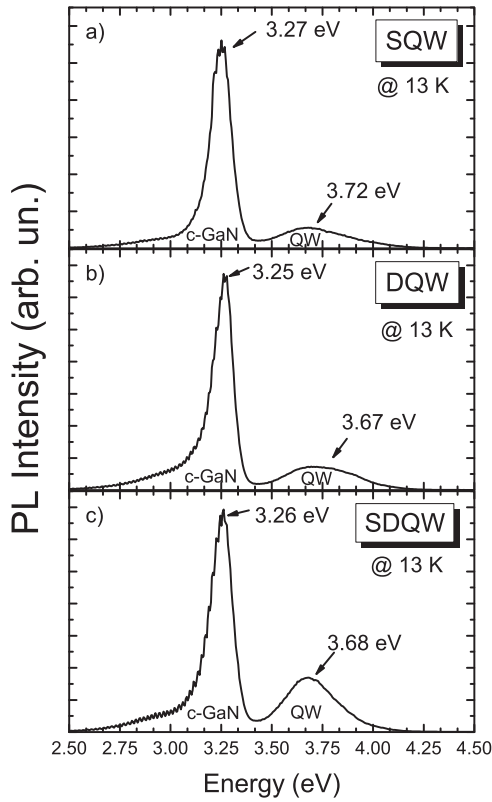


Fig. 3. PL spectra at 13 K under 266 nm excitation (a) SQU, (b) DQU and (c) SDQU.

Table 1
Full Width at Half Maximum of QWs emissions.

Samples	FWHM
SQU	~ 0.41 eV
DQU	~ 0.39 eV
SDQU	~ 0.30 eV

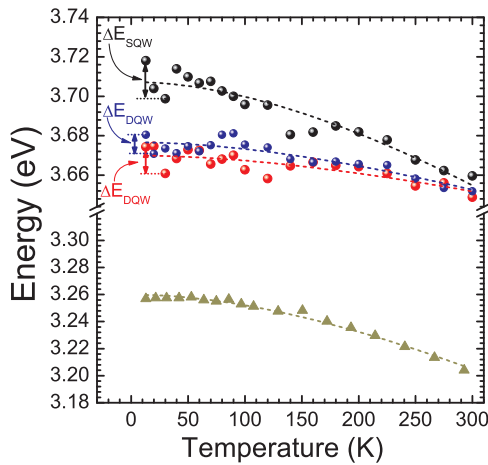


Fig. 4. The PL peak positions of QWs and reference sample (c-GaN bulk). The dashed lines correspond to the Varshni fitting.

detectable influence to interfaces defects.

The optical properties were investigated by photoluminescence spectroscopy in the temperature range of 13–300 K using a monochromator SPEX 270 M with a photomultiplier Hamamatsu Typ 943-02 and a 266 nm CW laser (CryLas FQCW 266) as excitation source.

Table 2
Parameter from Varshni fitting.

Sample	α (10^{-4} eV/K)	β (K)
SQU	5.21	595
DQU	1.82	602
SDQU	2.45	615
Reference	5.54	605

Table 3
Estimated values of localized states energies in low temperature.

Sample	Energy (meV)
SQU	$\approx 19 \pm 3$
DQU	$\approx 13 \pm 3$
SDQU	$\approx 10 \pm 3$

3. Results and discussion

Fig. 3 shows the PL spectra at 13 K for all structures. The peak around 3.27 eV corresponds to the excitonic emission of c-GaN [6] and the slight difference in the PL peaks between samples can be associated due to the fluctuations in Si-doping [15]. The peaks around 3.70 eV are the QWs emissions. The broad bands for QWs are attributed to mono-layers fluctuations during the growth process which are associated to interfaces defects.

Table 1 presents the value of the full width at half maximum (FWHM) for the QWs emissions. For a typical sample of undoped c-GaN at room temperature the exciton emission has a FWHM of about 117 meV [6]. For the QW emission we can note a decrease of the linewidth from SQU to the SDQU. The decrease in the FWHM can be related to the increase of the material quality [16,17]. In the QW structures, it can be attributed to the presence of intermediary AlN layer and mainly by the presence of the step structure.

The PL peak positions as function of temperature for the QWs and for a reference c-GaN bulk sample are shown in Fig. 4. The experimental data were fitted by Varshni equation [18]:

$$E_g(T) = E_g(0) - \frac{\alpha T^2}{\beta + T} \quad (1)$$

where $E_g(0)$ is the energy band gap at 0 K, α and β are empirical coefficients. The α parameter is related to the $\lim_{T \rightarrow \infty} \frac{dE}{dT}$ and β parameter has a value similar to the Debye temperature that is approximately 600 K for c-GaN [19]. Table 2 shows the fitting results whose values present a good correlation to the literature [19].

We notice that for temperatures above > 180 K the fitting has a good correlation with the experimental data. However, the position of emission peak fluctuates in low temperatures. This behavior is related to the localization effects at the interfaces of the quantum wells [20,21]. In our case, these fluctuations are related to the interface quality by the quantity ΔE defined by the deviation from the average value expected by Varshni fitting curve in Fig. 4. The values for these fluctuations are presented in Table 3. We note a decrease of ΔE from SQU as far an intermediate AlN layer is introduced between sequencing quantum well. The introduction of AlGaIn step layer also decreases the fluctuation associated to these interface-related localized states observed at low temperatures.

To complement this analysis, PL integrated intensities were plotted as a function of the reciprocal thermal energy in Fig. 5. Usually, this behavior is well modeled by the Arrhenius-like equation [6,22].

$$I(T) = \frac{I_0}{1 + C \exp\left(-\frac{E_a}{k_B T}\right)} \quad (2)$$

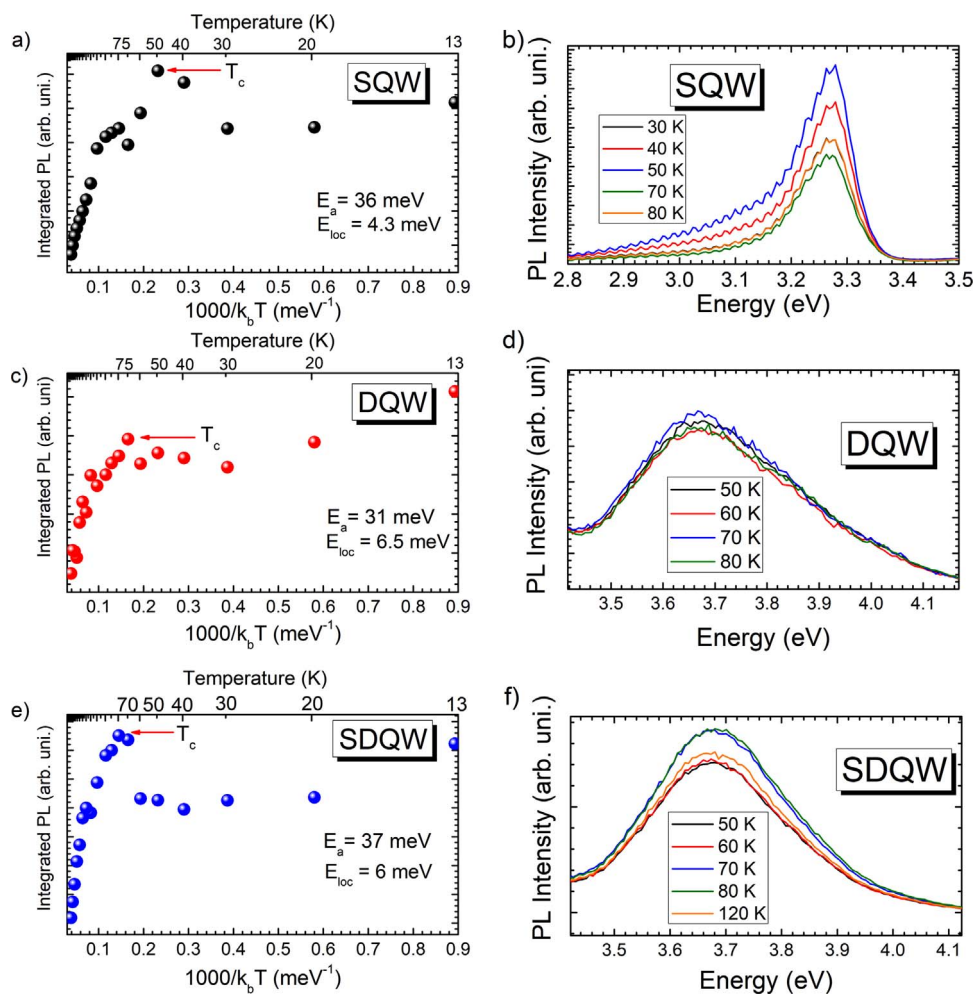


Fig. 5. The integrated PL intensities in (a), (c) and (e) show the influence of carrier localization related to interfaces. The PL spectra shown in (b), (d) and (f) confirm the anomalous increasing of intensities.

Table 4

Estimated energy of the localized states and the ionization energy of the exciton into the QW.

Sample	E_{loc} (meV)	E_a (meV)
SQW	4.3 ± 0.4	36
DQW	6.5 ± 0.4	31
SDQW	6.0 ± 0.4	37

where I_0 is the PL intensity at 0 K, C is the ratio between radiative and non-radiative lifetimes, E_a is the ionization energy for the exciton inside the QW and k_B is the Boltzmann constant.

In Fig. 5 the deviation from the expected tendency is notable that the intensities increase in a range of ascending temperatures between 30 and 80 K. This anomalous behavior was previously reported for traps localization in ZnO using a qualitative model based on potential fluctuations [23]. In our case, interface defects can be interpreted as potential fluctuations which trap the photocarriers at low temperature. Trapped carriers are released/thermally activated from local minima as temperature increases and recombine in the conventional way. The deepest fluctuation depth is defined by a critical temperature T_c , i.e. its energetic depth is $k_B T_c$. Above T_c the localization potentials due to interfacial defects are screened and the PL emission follows the expected decreasing as temperature increases. Considering $k_B T_c$ as the thermal energy for photocarriers avoiding this localization region, we define E_{loc} as the localization energy range and E_a as the exciton ionization energy obtained by Eq. (2). The results are depicted in Table 4.

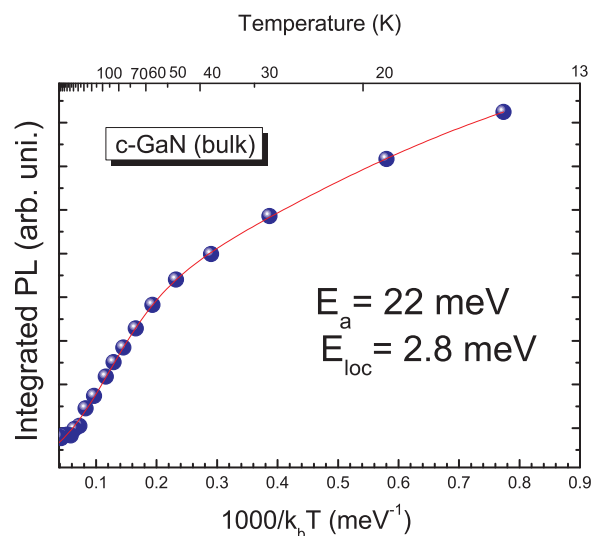


Fig. 6. Integrated PL Intensity as a function of $1000/k_B T$ for the c-GaN bulk sample.

Additionally, we analyzed the integrated PL intensity as a function of the reciprocal thermal energy for the c-GaN (bulk) in Fig. 6. For this case we introduce an Arrhenius expression with two non-radiative processes [21]: C_1 relative to the localized and C_2 relative to delocalized excitons, where the parameter (1) is related to the process predominant

at low temperatures and (2) at high temperatures:

$$I(T) = \frac{I_0}{1 + C_1 \exp\left(-\frac{E_{loc}}{k_b T}\right) + C_2 \exp\left(-\frac{E_a}{k_b T}\right)}, \quad (3)$$

We can notice that the activation energy is about 22 meV which is close to the exciton energy for the c-GaN [6] while a carrier localization in a shallow localized state is about 3 meV and could be due to native defects of c-GaN. We notice that the nature of QW localized states is different from the reference, which is bulk and has no interfaces. Their large values are comparable to the average $\Delta E/2$ of the fluctuation energies found in Table 3 and they are screened and contribute to PL up to the critical temperature. Additionally the larger excitonic ionization energies (E_a) are credited to the quantum confinement nature of QW structure.

These results indicate a better interface for the SDQW as compared to SQW and DQW which can be associated to the introduction of a AlN barrier (interlayer) in the QW. The AlN interlayer tends to decrease the superficial tension in the interfaces [24]. Besides that, the AlGaIn has a surfactant behavior [25,26] that contribute to the loss of interface roughness and the decreasing of localized states energy.

4. Conclusions

In conclusion, cubic GaN/(Al)GaN multiple quantum wells were grown by plasma assisted molecular beam epitaxy with three different configurations at interfaces. The investigation was based on temperature dependent photoluminescence which shows anomalous behavior at low temperatures. This behavior was attributed to carrier localization effects due to interface defects. Peak position and integrated intensity were analyzed and the obtained localization energies are correlated to the interfaces which shows smaller values when AlN is employed as intermediate layer. The interpretation method contributes to a fast diagnostic of interfacial defects as carrier localization centers.

Acknowledgements

LKSH thanks the support of CAPES “Programa de bolsa de doutorado no exterior - PDSE” (Process: BEX 11746/13-0) and FAPEMIG for the financial support. TW and DJA acknowledges financial support by the Deutsche Forschungsgemeinschaft (DFG) via TRR142 (Project B02) and by the Centre for Optoelectronics and Photonics Paderborn (CeOPP).

References

- [1] L.M.A. Tolbert, B.A. Ozpineci, S.K.A. Islam, M.S.A. Chinthavali, Wide Bandgap Semiconductors for Utility Applications in: Proceedings of the IASTED International Conference on Power and Energy Systems, Palm Springs, California, 2003, pp. 317–321.
- [2] A. Yoshikawa, H. Matsunami, Y. Nanishi, Development and applications of wide bandgap semiconductors, in: K. Takahashi, A. Yoshikawa, A. Sandhu (Eds.), Wide Bandgap Semiconductors: Fundamental Properties and Modern Photonic and Electronic Devices, Springer, Berlin, Heidelberg, Berlin, 2007, pp. 1–24.
- [3] A.R. Acharya, Group III – nitride semiconductors: preeminent materials for modern electronic and optoelectronic applications, *Himal. Phys.* 5 (2015) 5.
- [4] M. Deppe, J.W. Gerlach, D. Reuter, D.J. As, Incorporation of germanium for n-type doping of cubic GaN, *Phys. Status Solidi (B)* 254 (2017) 1600700.
- [5] T. Wecker, T. Jostmeier, T. Rieger, E. Neumann, A. Pawlis, M. Betz, D. Reuter, D.J. As, Linear and nonlinear behaviour of near-IR intersubband transitions of cubic GaN/AlN multi quantum well structures, *J. Cryst. Growth* (2017).
- [6] D.J. As, F. Schmilgus, C. Wang, B. Schöttker, D. Schikora, K. Lischka, The near band edge photoluminescence of cubic GaN epilayers, *Appl. Phys. Lett.* 70 (1997) 1311–1313.
- [7] D.J. As, C. Mietze, MBE growth and applications of cubic AlN/GaN quantum wells, *Phys. Status Solidi (A)* 210 (2013) 474–479.
- [8] A. Radosavljević, J. Radovanović, V. Milanović, D. Indjin, Cubic GaN/AlGaIn based quantum wells optimized for applications to tunable mid-infrared photodetectors, *Opt. Quantum Electron.* 47 (2015) 865–872.
- [9] A.D. Rodrigues, M.P.F. de Godoy, C. Mietze, D.J. As, Phonon localization in cubic GaN/AlN superlattices, *Solid State Commun.* 186 (2014) 18–22.
- [10] P. Chen, R. Zhang, Z.M. Zhao, D.J. Xi, B. Shen, Z.Z. Chen, Y.G. Zhou, S.Y. Xie, W.F. Lu, Y.D. Zheng, Growth of high quality GaN layers with AlN buffer on Si(1 1 1) substrates, *J. Cryst. Growth* 225 (2001) 150–154.
- [11] J. Schörmann, S. Potthast, D.J. As, K. Lischka, In situ growth regime characterization of cubic GaN using reflection high energy electron diffraction, *Appl. Phys. Lett.* 90 (2007) 041918.
- [12] T. Schupp, K. Lischka, J. Schoermann, E. Tschumak, M.P.F. de Godoy, K. Lischka, Molecular beam epitaxy of nonpolar cubic AlxGa1-xN/GaN epilayers, *Mater. Res. Soc. Symp. Proc.* 1040 (2008).
- [13] T. Schupp, K. Lischka, D.J. As, MBE growth of atomically smooth non-polar cubic AlN, *J. Cryst. Growth* 312 (2010) 1500–1504.
- [14] H. Machhadani, M. Tcherynecheva, S. Sakr, L. Rigutti, R. Colombelli, E. Warde, C. Mietze, D.J. As, F.H. Julien, Intersubband absorption of cubic GaN/Al(GaN) quantum wells in the near-infrared to terahertz spectral range, *Phys. Rev. B* 83 (2011) 075313.
- [15] J.R.L. Fernandez, C. Moysés Araújo, A. Ferreira da Silva, J.R. Leite, Bo.E. Sernelius, A. Tabata, E. Abramof, V.A. Chitta, C. Persson, R. Ahuja, I. Pepe, D.J. As, T. Frey, D. Schikora, K. Lischka, Electrical resistivity and band-gap shift of Si-doped GaN and metal-nonmetal transition in cubic GaN, InN and AlN systems, *J. Cryst. Growth* 231 (2001) 420–427.
- [16] G.D. Gilliland, Photoluminescence spectroscopy of crystalline semiconductors, *Mater. Sci. Eng.: R. Rep.* 18 (1997) 99–399.
- [17] C. Lamberti, G. Agostini, Characterization of Semiconductors Heterostructures and Nanostructures, Elsevier, Netherlands, 2013.
- [18] Y.P. Varshni, Temperature dependence of the energy gap in semiconductors, *Physica* 34 (1967) 149–154.
- [19] S.J. Xu, C.T. Or, Q. Li, L.X. Zheng, M.H. Xie, S.Y. Tong, H. Yang, Defect states in cubic GaN epilayer grown on GaAs by metalorganic vapor phase epitaxy, *Phys. Status Solidi (A)* 188 (2001) 681–685.
- [20] S.A. Lourenço, M.D. Teodoro, P.P. González-Borrero, I.F.L. Dias, J.L. Duarte, E. Marega Jr, G.J. Salamo, Analysis of confinement potential fluctuation and band-gap renormalization effects on excitonic transition in GaAs/AlGaAs multiquantum wells grown on (1 0 0) and (3 1 1)A GaAs surfaces, *Phys. B: Condens. Matter* 407 (2012) 2131–2135.
- [21] V. Lopes-Oliveira, L.K.S. Herval, V. Orsi Gordo, D.F. Cesar, M.P.F. de Godoy, Y. Galvão Gobato, M. Henini, A. Khatib, M. Sadeghi, S. Wang, M. Schmidbauer, Strain and localization effects in InGaAs(N) quantum wells: tuning the magnetic response, *J. Appl. Phys.* 116 (2014) 233703.
- [22] Y. Fang, L. Wang, Q. Sun, T. Lu, Z. Deng, Z. Ma, Y. Jiang, H. Jia, W. Wang, J. Zhou, H. Chen, Investigation of temperature-dependent photoluminescence in multi-quantum wells, *Sci. Rep.* 5 (2015) 12718.
- [23] Y.J. Onofre, S. de Castro, M.P.F. de Godoy, Effect of traps localization in ZnO thin films by photoluminescence spectroscopy, *Mater. Lett.* 188 (2017) 37–40.
- [24] L.M. Sorokin, A.E. Kalmykov, V.N. Bessolov, N.A. Feoktistov, A.V. Osipov, S.A. Kukushkin, N.V. Veselov, Structural characterization of GaN epilayers on silicon: effect of buffer layers, *Tech. Phys. Lett.* 37 (2011) 326–329.
- [25] C. Adelmann, E. Sarigiannidou, D. Jalabert, Y. Hori, J.-L. Rouvière, B. Daudin, S. Fanget, C. Bru-Chevallier, T. Shibata, M. Tanaka, Growth and optical properties of GaN/AlN quantum wells, *Appl. Phys. Lett.* 82 (2003) 4154–4156.
- [26] G. Mula, C. Adelmann, S. Moehl, J. Oullier, B. Daudin, Surfactant effect of gallium during molecular-beam epitaxy of GaN on AlN (0001), *Phys. Rev. B* 64 (2001) 195406.